

Testing the polarisation mode of GWB-II using two LO-schemes in the GAB system

Dharam V. Lal

dharamATncraDOTtifrDOTresDOTin

November 3, 2014

Contents

1 Overview	2
2 Motivations	2
3 Data	2
3.1 Tests at 1280 MHz band	3
3.2 Tests at 1390 MHz band	3
4 Summary	6
5 Future directions	6

List of Figures

1 Amplitude and phase obtained for 3C 286 at the 1280 MHz sub-bands of L-band as a function of time for two LO-lock schemes.	4
2 Amplitude and phase obtained for 3C 286 at the 1390 MHz sub-bands of L-band as a function of time for two LO-lock schemes.	5
3 Amplitude and phase obtained for 3C 48 at the 1230 MHz as a function of time for two LO-lock schemes.	7
4 Amplitude and phase obtained for 3C 48 at the 1450 MHz as a function of time for two LO-lock schemes.	8
5 Amplitude and phase obtained for 3C 48 at the 1450 MHz as a function of time.	9

List of Tables

1 GMRT test data presented in this report.	2
--	---

1 Overview

This report focuses on testing the polarisation mode of GWB-II (GMRT Wideband Backend ver. II). Since, two LO-lock schemes, synthesiser and signal-generator modes are available at the L-band, we record data from both LO-lock schemes in the GAB (GMRT analog baseband) and use GSB data as the benchmark. Similar to our several previous tests, here along with the use of cross-correlation count, ccf^1 , for a baseline at a given frequency as a function of time, we also use phase as a function of time as a measure of stability/performance of the GWB-II.

This report is organised as follows. Section 2 explains the motivations and Section 3 explains methodology of these tests. A summary of results of the analysis are presented in subsequent Sections, namely, 3.1 and 3.2 show results obtained at the two (of the four) sub-bands, 1280 MHz and 1390 MHz of the L-band using both modes of the LO-lock schemes, respectively. We summarise our findings in Section 4, and make some final concluding remarks with regard to testing of ‘full polar’ mode of GWB-II using both LO schemes.

2 Motivations

The motivation of this report is simple, to test the polarisation mode of GWB-II as one of the standard interferometric observation mode via. two LO-lock schemes, synthesiser and signal-generator that are available at the L-band. The results from these findings for two (of the four) sub-bands, 1280 MHz and 1390 MHz of the L-band are summarised in Section 4.

3 Data

GMRT data using new GWB-II, which is acquired using the new GMRT analog baseband (GAB) chain at two sub-band frequencies of L-band was acquired in order to understand the performance of GWB-II and its comparison with the existing GSB. The observing log for the test data presented in this report is shown in Table 1.

Table 1: GMRT test data presented in this report.

Frequency	Obs. Date	Target	Expected ccf
1390 MHz	2014-10-16	3C 286	0.055
1280 MHz	2014-10-16	3C 286	0.055

Since, these are an upgrade related tests of GMRT to understand varying ccf scales from GWB on various baselines with respect to the GSB, (i) both, broadband system and related antennas are a must and (ii) data from GWB and GSB needs to be recorded simultaneously. These observations were made in the default mode for ‘full polar’ mode. For projects requiring imaging in Stokes Q and U, the instrumental polarization should be determined through observations of a bright calibrator source spread over a range in parallactic angle. In addition, a single scan that would give sufficient SNR of a bright unpolarised unresolved

¹The ccf from a point/calibrator source with flux density, $S\nu$ is defined as

$$\text{ccf} = \frac{G \times S\nu}{T_{\text{sys}}},$$

where G and T_{sys} are Gain (in K Jy^{-1}) and system temperature (in K) of a GMRT antenna, respectively.

source, known to have very low polarization) is necessary to determine the leakage terms. For GMRT, we do not have these calibration statistics, including time dependent instrumental polarization. Therefore, we observed 3C 286 source (Table 1), and because it is 9.5% (at 1450 MHz) polarised at these frequencies, we assume that some small fraction of the expected ccf obtained in the total intensity mode of observations.

Data was acquired from these tests, which were performed at the two of the four sub-bands of the L-band to understand (i) the variation of ccf (or amplitude) and phase as a function of time in GWB-II as compared to the GSB for the two, ‘synthesiser’ and ‘signal-generator’ based LO-schemes. The results from it are presented below.

3.1 Tests at 1280 MHz band

Fig. 1 presents results for the 1280 MHz band. As mentioned above these observations were made using the default settings of the GWB-II for the ‘full polar’ mode. Plots show cross-polar products (product of channel-1 of reference antennas and channel-2 of the other antenna, etc.). The ccfs (or the amplitudes) and the phases as a function of time for GSB (left panel) and for GWB-II (right-panel) data are shown.

Briefly, Fig. 1 shows that both ccf (or amplitude) and the phase as a function of time for the GWB-II compare well with the ccf (or amplitude) and the phase as a function of time for the GSB. This behaviour is seen for both , ‘synthesiser’ and ‘signal-generator’ based LO-schemes.

3.2 Tests at 1390 MHz band

Fig. 2 presents results for the 1390 MHz band. As mentioned above these observations too were made using the default settings of the GWB-II for the ‘full polar’ mode. Plots show cross-polar products (product of channel-1 of reference antennas and channel-2 of the other antenna). The ccfs (or the amplitudes) and the phases as a function of time for GSB (left panel) and for GWB-II (right-panel) data are shown.

Briefly, Fig. 2 shows that both ccf (or amplitude) and the phase as a function of time for the GWB-II compare well with the ccf (or amplitude) and the phase as a function of time for the GSB. This behaviour is seen for both , ‘synthesiser’ and ‘signal-generator’ based LO-schemes.

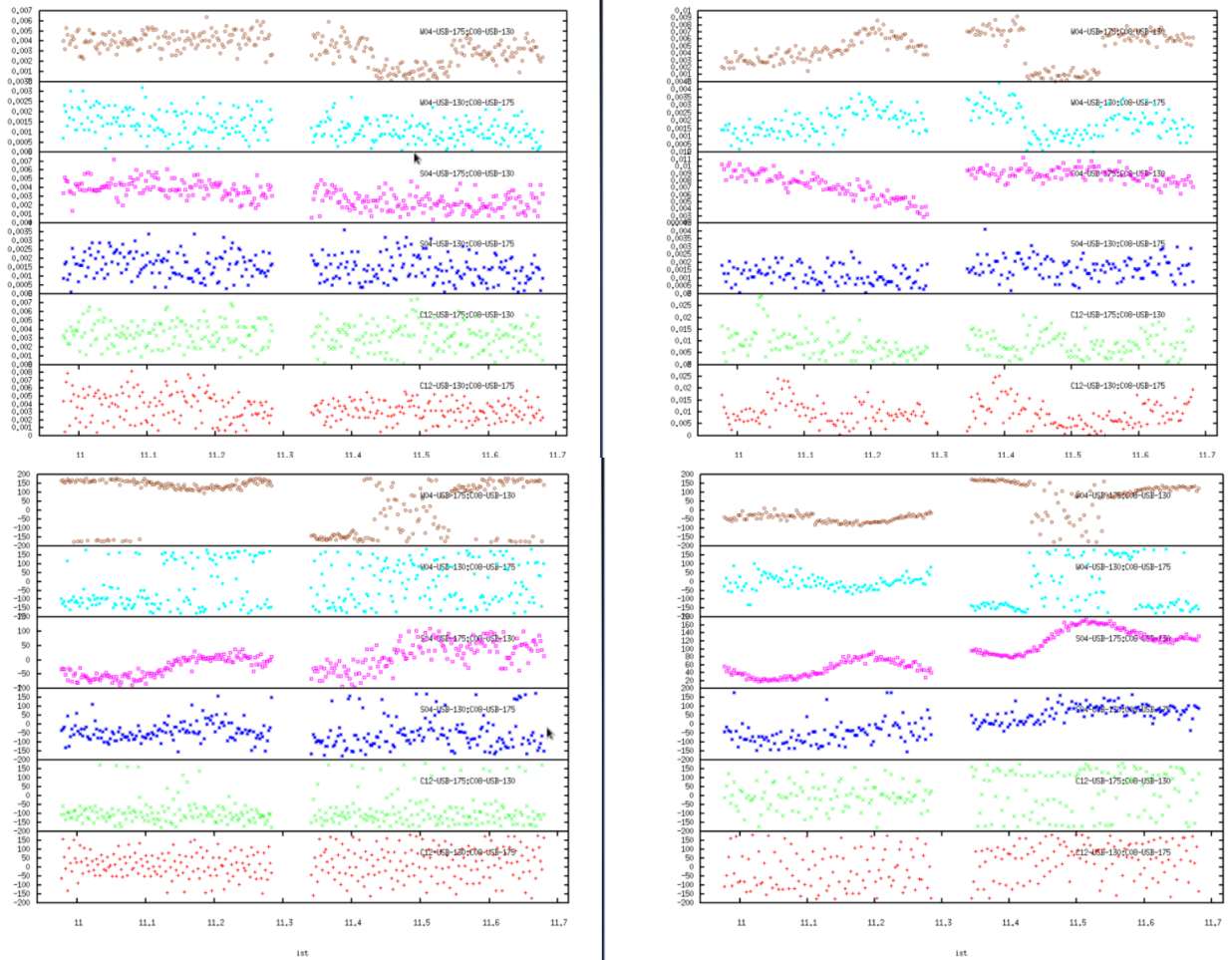


Figure 1: Plot showing ccfs (amplitudes) (upper panel) and phases (lower panel) as a function of time for a channel at the centre of the 1280 MHz frequency band. Note (i) in both panels, left is GSB and right is GWB data, (ii) the channels (channel-128 in the left panel and channel-638 in the right panel, respectively) are chosen such that they correspond to the same frequency, and (iii) for the data from GWB-II (right panel), the left-scan correspond to the ‘synthesiser’ and the right-scan correspond to the ‘signal-generator’ mode of LO lock schemes.

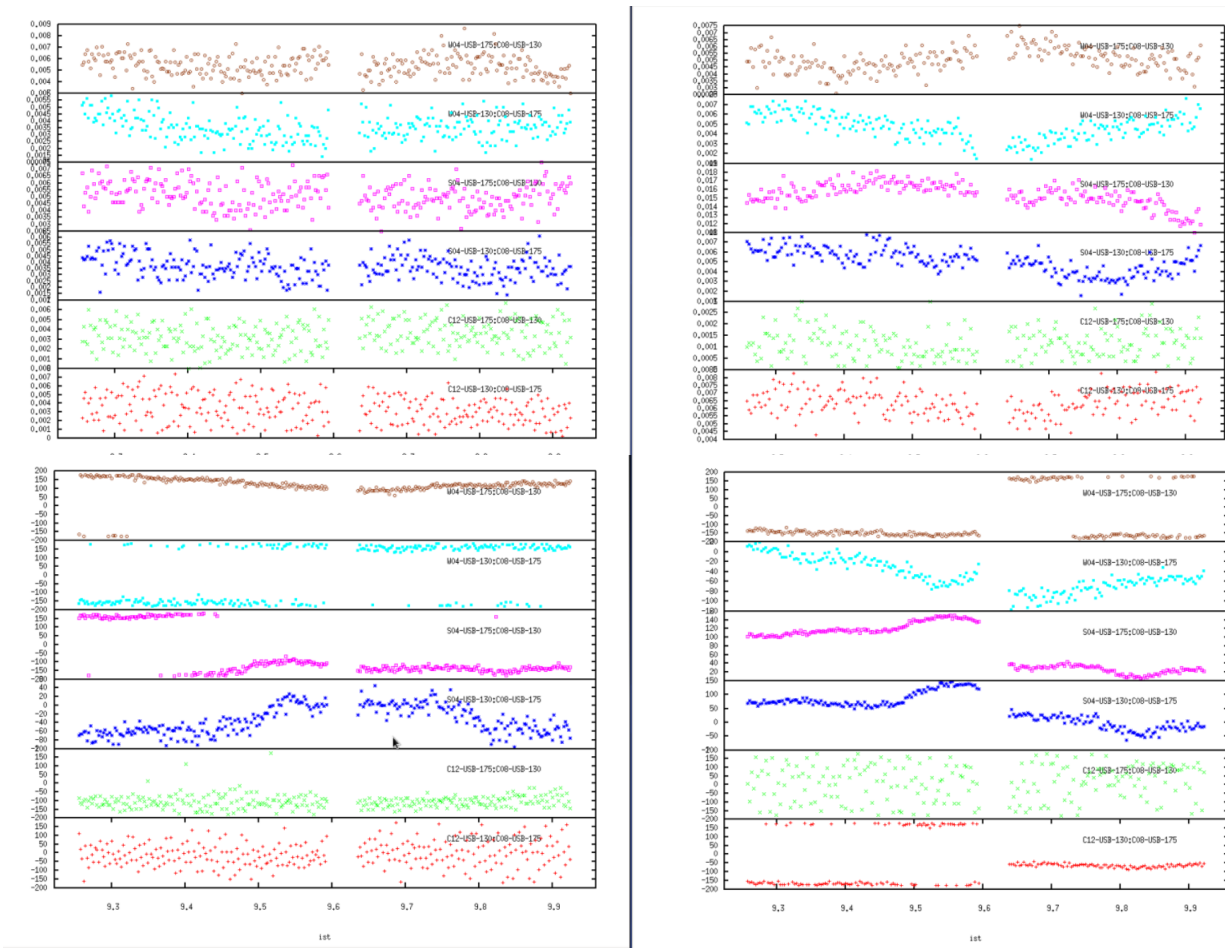


Figure 2: Plot showing ccf (amplitudes) (upper panel) and phases (lower panel) as a function of time for a channel at the centre of the 1390 MHz frequency band. Note (i) in both panels, left is GSB and right is GWB-II data, (ii) the channels (channel-128 in the left panel and channel-638 in the right panel, respectively) are chosen such that they correspond to the same frequency, and (iii) for the data from GWB-II (right panel), the left-scan correspond to the ‘signal-generator’ and the right-scan correspond to the ‘synthesiser’ mode of LO lock schemes.

4 Summary

Based on results presented above in Sections 3.1 and 3.2, here we quantify these results. The related plots give qualitative faithful match, and it also compares results from the two LO-lock schemes, synthesiser and signal-generator modes that are now available at these two sub-bands of the L-band. Our conclusions from these new observations can be summarised as follows.

- i Both sub-bands of the L-band show that both ccf (or amplitude) and the phase as a function of time for the GWB-II compare well with the ccf (or amplitude) and the phase as a function of time for the GSB.
- ii The scatter/fluctuation in the GWB-II data, both in amplitude and phase is lower as compared to the GSB.
- iii The GWB-II data from the two sub-bands, 1280 and 1390 MHz of the L-band from both LO-lock schemes, ‘synthesiser’ and ‘signal-generator’ behave as expected and there is no appreciable/noticeable change between these two LO-lock schemes for the two (of the four) sub-bands of the L-band.

The results presented below in Appendix for the 3C 48 source also give similar consistency.

5 Future directions

Below, we list our some of the tests that we plan in future in order to address the following issues:

- We propose to repeat these test once again and include other two sub-bands of the L-band in order to (i) test the long term stability of the system and (ii) obtain data for all four sub-bands in a consistent and an identical manner/setup.
- As discussed in Section 3 the instrumental poalarisation and the leakage of poalarisation are important. Hence in subsequent test, more deep observations should be made to quantify these two effects along with the time dependent instrumental polarization at an appropriate sensitivity level.

Acknowledgments

DVL thanks (i) all the members of the GMRT backend and OF teams, operators for the support and help, and for making these observations, and (ii) Prof. Y. Gupta for several useful conversations and for contantly reminding me to bring this exercise to a logical completion. We thank the staff of the GMRT that made these observations possible. GMRT is run by the National Centre for Radio Astrophysics of the Tata Institute of Fundamental Research.

Appendix

Below, we present results from an old observation made on 2014-09-17 of the 3C 48 source using the ‘full polar’ mode of the GWB-II using default settings. The observations were made at 1450 MHz (Fig. 3) and at 1230 MHz (Fig. 4) RF, respectively, which uses both LO-lock schemes, synthesiser and signal-generator modes in the GAB that are available at the sub-bands of the L-band. In addition, a 2 hr long run observation was also made for the source using the ‘synthesiser’ mode of LO-lock scheme (see Fig. 5). Hereagain, we record data from the GSB as the benchmark.

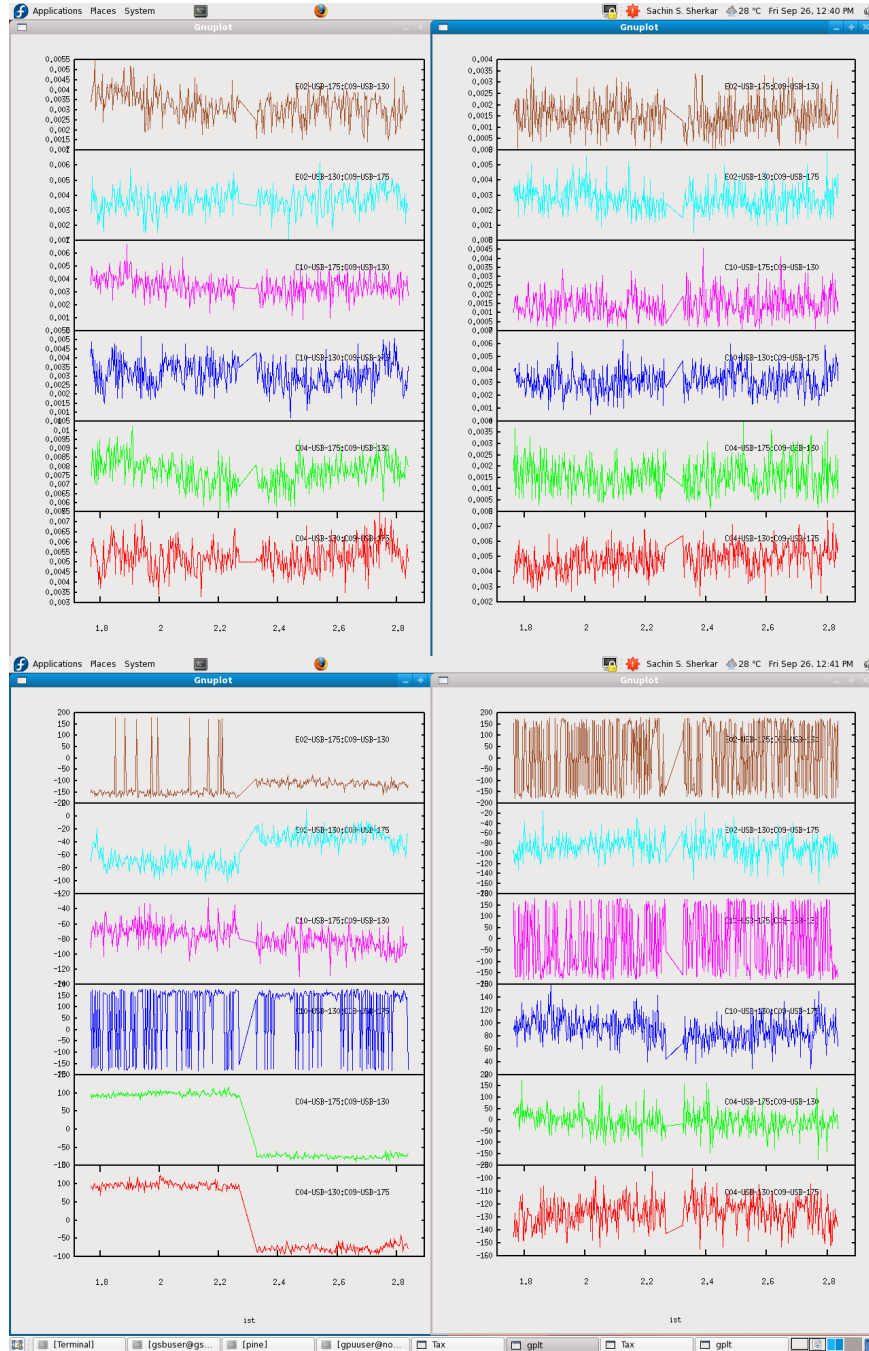


Figure 3: Plot showing ccfs (amplitudes) (upper panel) and phases (lower panel) as a function of time for a channel at the centre of the 1230 MHz (= RF) frequency band. Note (i) in both panels, left is GWB-II and right is GSB data, and (ii) for the data from GWB-II (left-panel), the left-scan correspond to the 'signal-generator' and the right-scan correspond to the 'synthesiser' mode of LO lock schemes.

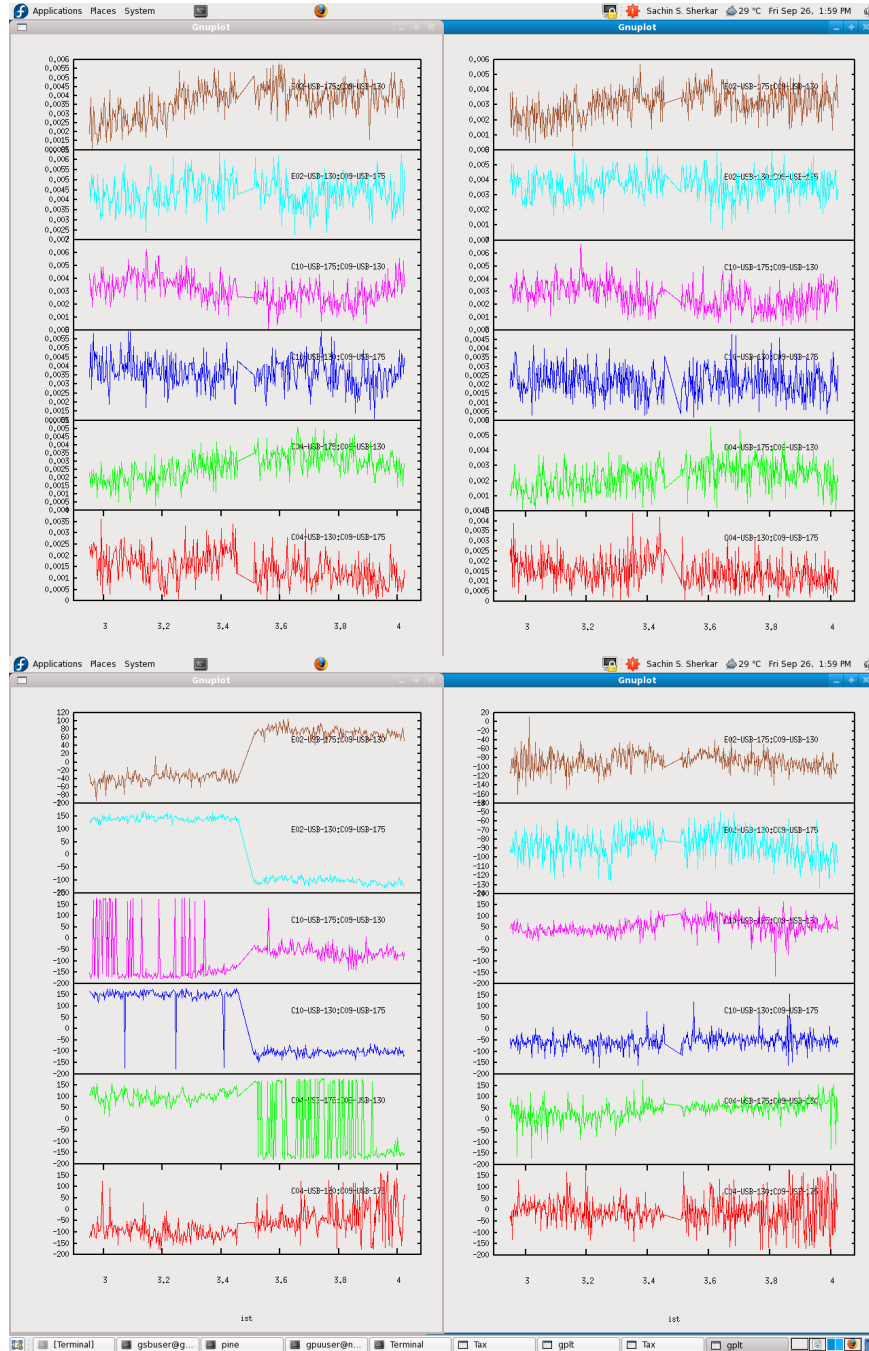


Figure 4: Plot showing ccfs (amplitudes) (upper panel) and phases (lower panel) as a function of time for a channel at the centre of the 1450 MHz (= RF) frequency band. Note (i) in both panels, left is GWB-II and right is GSB data, and (ii) for the data from GWB-II (left-panel), the left-scan correspond to the ‘signal-generator’ and the right-scan correspond to the ‘synthesiser’ mode of LO lock schemes.

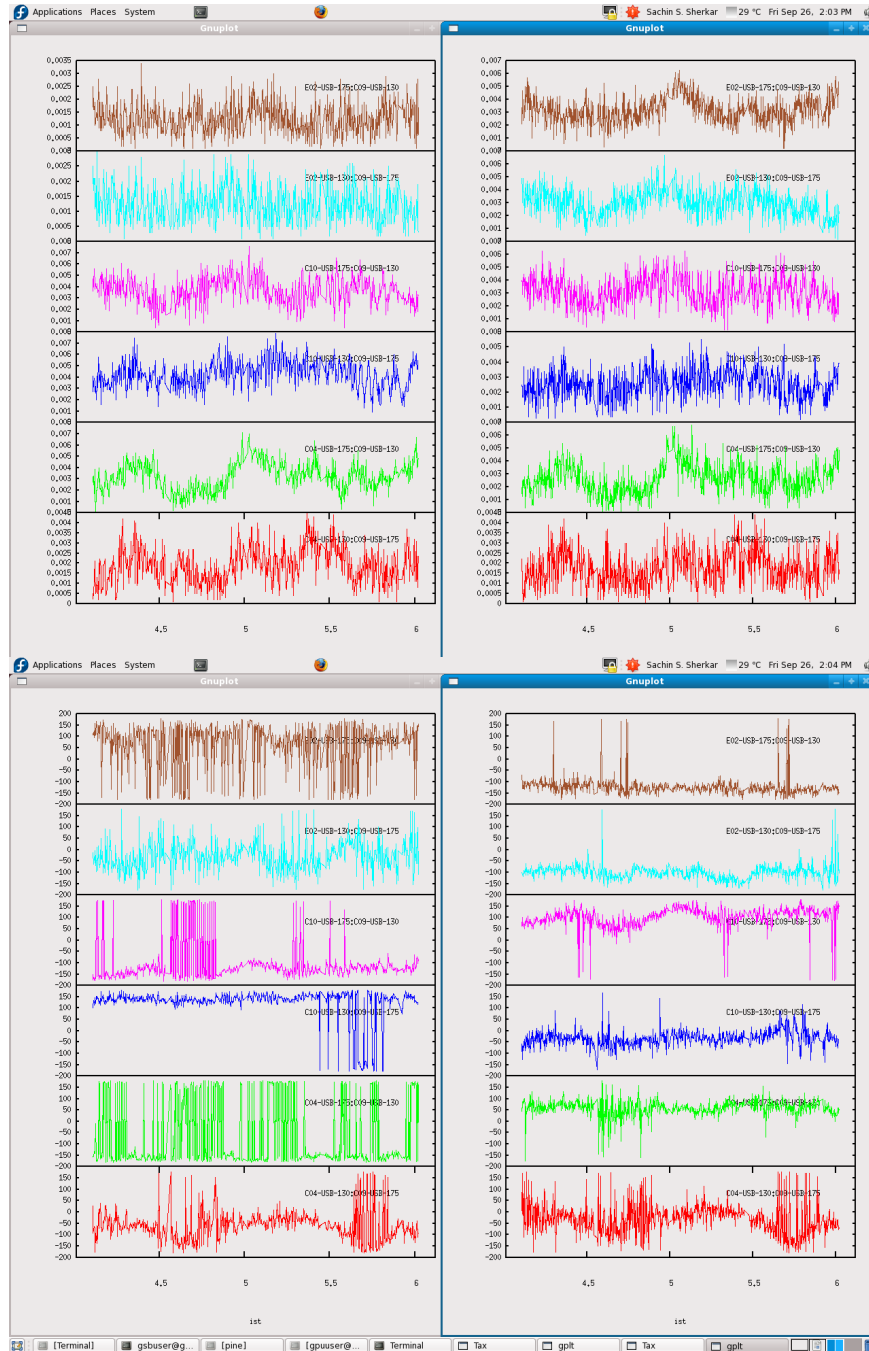


Figure 5: Plot showing ccfs (amplitudes) (upper panel) and phases (lower panel) as a function of time for a channel at the centre of the 1450 MHz (= RF) frequency band. Note in both panels, left is GWB-II and right is GSB data and uses the 'synthesiser' mode of LO lock scheme.